Peer-to-Peer Netw. Appl. (2016) 9:616–627
DOI 10.1007/s12083-015-0331-5

A reliable QoS-aware routing scheme for neighbor area network in smart grid

Xiaoheng Deng · Lifang He · Xu Li · Qiang Liu · Lin Cai · Zhigang Chen

Received: 21 October 2014 / Accepted: 26 January 2015 / Published online: 19 February 2015

Abstract A reliable bi-directional communication network is one of the key factors in smart grid (SG) to meet application requirements and improve energy efficiency. As a promising communication infrastructure, wireless mesh network (WMN) can provide high speed and cost-effect communication for SG. However, challenges remain to maintain high reliability and quality of service (QoS) when applying WMNs to SG. In this paper, we first propose a hybrid wireless mesh protocol (HWMP) based neighbor area network (NAN) QoS-aware routing scheme, named HWMP-NQ, to meet the QoS requirements by applying an integrated routing metric to route decision with effective link condition probing and queue optimization. To further improve the reliability of the proposed HWMP-NQ, we present a multi-gateway backup routing scheme along with a routing reliability correction factor to mitigate the impact of routing oscillations. Finally, we evaluate the performances of the proposed schemes on NS3 simulator. Extensive simulations demonstrate that HWMP-NQ can distinguish different applications and satisfy the QoS requirements respectively, and also improve the average packet delivery ratio and throughput with a reduced routing overhead, even with a high failure rate of mesh nodes.

X. Deng (✉) · L. He · X. Li · Q. Liu · Z. Chen
School of Information Science and Engineering, Central South University, Changsha, People's Republic of China
e-mail: dxh@csu.edu.cn

L. Cai
Department of electrical and Computer Engineering, University of Victoria, Victoria, Canada
e-mail: cai@ece.uvic.ca

Keywords Smart grid · Wireless mesh network · Neighbor area network · QoS

1 Introduction

Instant and reliable data transmission from power supplier to customers is of great significance in smart grid applications. With the driving force from industry, the SG has developed from one-way communication system of Automated Meter Reading (AMR) to bi-directional communication system of Advanced Metering Infrastructure (AMI) [1]. AMI integrates sensors, smart meters, data management system and monitor system to collect and distribute information between smart meters and grid facilities [2]. In addition, smart meters can control electric appliances through bi-directional communication between the smart meters and the AMI, and help users adjust electricity consumption to avoid usage peak and improve resource allocation. SG communication infrastructure consists of three different networks. These networks are home area network (HAN), neighborhood area network (NAN) and wide area network (WAN). A HAN focuses on small-scale data communication between devices inside typical households, and wireless sensor networks (WSNs) can be an appropriate candidate for it for energy efficiency improvement and network lifetime elongation [3–6]. A NAN is defined to provide a backbone for data that are transmitted from multiple HANs as well as providing various services of its own, possible communication technology for NANs would be IEEE 802.11 s, broadband power line communications (BPLC). While a WAN connects grid control centers and NAN data concentrators with long distance in very large areas, and transmits data in a very high-speed manner. Underlying technologies may significantly vary based on the implementation. As far as the wireless technologies are concerned, such as WiMax, 3GPP, Mesh could be used for WAN.

The neighbor area network (NAN) which forms data transmission bridges between utility backbone and households in SG. It is one of the most important parts in power grid that contributes to the safety and efficiency of the whole grid. High reliability and QoS of NAN communications are critically required [7–9]. Multi-hop wireless mesh network (WMN) based on IEEE 802.11 s can be a promising candidate for NAN since it can provide high-speed and reliable wireless data transmission in communication [10]. However, there are some challenges in hybrid wireless mesh protocol (HWMP) of WMN in respect of reliability and QoS when applying it to SG. First, the default airtime cost metric of HWMP uses fixed test frames, which does not consider different traffic situations of SG, and it may not be appropriate in some particular SG environment. Moreover, frequent routing oscillations and unstable route maintenance mechanism of HWMP both increase the routing overhead and reduce the available bandwidth, which significantly endangers the reliability of smart grid networks.

In this paper, we first propose HWMP-NQ, a HWMP based NAN QoS-aware routing scheme, to ensure QoS of different smart grid applications. By taking into account packet size and transmission rate, the airtime cost metric of HWMP is optimized to better reflect real-time routing cost. We also adopt a traffic QoS calculation algorithm based on single measurement to reduce the overhead of link measurements, and meet the QoS requirements of NAN through the QoS-based service differentiation strategy, which distinguishes different applications before transmission by considering the data size and QoS demands of different traffic situation. We also present a multi-gateway backup routing scheme with a routing reliability correction factor to mitigate routing oscillations to further improve the reliability of HWMP-NQ. Moreover, a single-hop path error (PERR) based routing maintenance mechanism is proposed, which helps reduce the routing overhead when link failure occurs. We implement the HWMP-NQ on ns-3 with various smart grid applications. Performance evaluations with high failure rate of mesh nodes are also provided. Simulation results demonstrate that the proposed schemes are superior in enhancing the reliability and meeting QoS requirements of smart grid systems, even with a high failure rate of wireless mesh nodes.

The reminder of this paper is organized as follows. In section 2, we review the related work of the research area. Then, we propose the HWMP-NQ routing scheme in section 3 and optimize the routing reliability of HWMP-NQ in section 4. Simulation results are provided in section 5. Finally, section 6 concludes this paper.

2 Related work

In the literature, several studies have been proposed to improve the reliability and QoS of smart grid communication system [11–21]. To derive the QoS requirements, a QoS mechanism called Optimized Multi-Constrained Routing (OMCR) is proposed in [11], which analyzed the dynamics of power market and the impact of communication metrics like delay and outage on the revenue of home appliances to guarantee the reliability of NAN. Gui and Liu proposed a new distributed topology control algorithm based on optimization of delay and energy [12], which sufficiently considers the interference degree and resources of nodes. The delay performance is guaranteed to satisfy the demand of network applications. In [14], the authors modeled the SG networks and presented the communication delay analysis in typical wireless network deployment scenarios of smart grid with Voronoi diagram, which provides theoretical guiding rules for designing WMN to meet the delay requirements.

With the fading and interference of wireless channel, link condition may vary frequently in WMN. Besides, interference from environment can also result in routing instability. Therefore, it is important to enhance routing reliability by providing alternative paths. Authors in [15] proposed Distributed Autonomous Depth-first Routing (DADR), a new distributed distance-vector routing protocol, which can adapt to changing link conditions quickly and minimize network control overhead at the same time. With DADR, when a link fails, packets will be transmitted through an alternate next hop, and the information of failed link is propagated with the packets. Therefore, routes are updated dynamically with little overhead. With Hydro, a hybrid routing protocol that combines local agility with centralized control [16], nodes within the network use distributed DAG formation to provide multiple routes, which are based on ETX [18], to border routers. A tree-based mesh routing scheme based on multi-gateway mesh network architecture is presented in [19]. The multi-gateway mesh routing scheme is based on a flexible mesh network architecture that expands on the hybrid tree routing of the IEEE802.11 s. They also proposed a packet scheduling scheme based on back-pressure to balance the traffic load among gateways. In addition, in [20, 21], the main issues of IEEE802.11 s reliability in SG communication network are analyzed and improved by modifying the routing metric, routing discovery and maintenance mechanism of HWMP.

Improving the measurement accuracy of HWMP routing metric is helpful to decrease the probability of routing oscillations, but its routing metric is not suitable for specific SG before optimizing it for various SG applications. Using historical records to help selecting a path can reduce the frequency of routing switching, while it does not consider different types of traffic flows that being processed in the router currently. When the backup routes are idle without any data to transmit or the primary route transmits the set and other types of application traffic simultaneously, it will still lead to unnecessary route switching. Therefore, we optimize the routing metric and design traffic differentiation strategy by considering different packet size and transmission rate. Then the frequency of route oscillations is reduced and the routing stability is improved by using historical route information in lower layer to revise historical routing information.

3 QoS optimization for SG applications

In NAN, various applications (control information, periodic power quality monitoring, meter reading and video surveillance, etc.) have different QoS requirements in terms of packet size, frequency, delay, jitters and bandwidth, which should be considered in the routing protocol design. In this section, we propose a HWMP based NAN QoS-aware routing protocol called HWMP-NQ to meet the QoS requirements of SG applications by including the data size and the transmission rate in airtime cost metric of HWMP.

3.1 Routing metric optimization

In NAN, various applications are transmitted simultaneously with different QoS requirements and packet size. For example, meter reading information and power quality monitoring information have smaller packet size, and can tolerate relatively longer delay. On the other hand, the packet size of control information and on-demand response flow is larger and has higher latency and reliability requirements. In order to ensure the QoS requirements for various applications, we modify the airtime cost of HWMP by considering the data size and transmission rate as Eq. (1):

$$C_a = \left(O_{ca} + O_p + \frac{B_t}{R_1}\right)\frac{1}{1-e_f(B_t, R_1)} \tag{1}$$

where B_t is the test frame size, R_1 is the data rate, which is set to 1Mbps as default in the HWMP, and $e_f(B_t, R_1)$ is the frame error rate with test frame size B_t and transmission rate of test frame R_1. We use the number of retransmissions to calculate the failure rate of the current network, which is shown as:

$$e_f(B_t, R_1) = \frac{\frac{1}{P}\sum_{i=1}^{P} M_i}{RT_{\max}} \tag{2}$$

where M_i is the number of attempted MAC level retransmissions for frame i, is the total number of successful and failed frame transmissions, and $RT_{\max}$ is the maximum allowed retransmission count.

The larger packet size and higher transmission rate are, the lower successful transmission ratio is, so IEEE 802.11 devices usually employ adaptive rate mechanism in MAC layer and use channel conditions to adjust the rate for current packets. We modify the airtime cost metric by considering packet size and transmission rate:

$$C_a(ps) = \left(O_{ca} + O_p + \frac{ps}{R_i}\right)\frac{1}{1-e_f(ps, R_i)} \tag{3}$$

where ps is the data size, R_i is the transmission rate with i modulation mode, it relates to the IEEE 802.11 standard (802.11b is 11Mbp, and 802.11a is 54Mbps) and adopted rate adjustment mechanism, $e_f(ps, R_i)$ is the error rate when data size is ps and transmission rate is R_i. We do not consider the selection of R_i, because it can be included into routing criterion calculation after rate selection by the link-layer adaptive rate algorithm. Therefore, $C_a(ps)$ can be used with different adaptive rate algorithms and has a good compatibility.

3.2 QoS calculation for SG applications

In order to calculate the $C_a(ps)$, we need to obtain the error rate under different data size and transmission rate. In IEEE 802.11 s, the detecting frame is sent by broadcasting, so each time only one rate and one frame size capsR_1n be measured. If employing direct measurement method, it can be obtained through calculating the average value of several broadcasted detecting frames. But this will greatly increase the link measurement overhead. As the IEEE 802.11 a/b have 12 rates, it will result in the overhead and increase the probability of channel collision, if we need to measure each rate separately.

Algorithm1. Frame error rate calculation algorithm based on single measurement.

Input: the test frame error rate $e_f(B_t, R_1)$, the test frame size B_t, the test frame rate R_i, the packet size ps and the data transmission rate R_1;

Output: the frame error rate $e_f(ps, R_i)$.

1. snr = findSNR ($e_f(B_t, R_1)$, B_t, R_1)
2. $e_f(ps, R_i)$ = findFER (snr, ps, R_i)
3. Return $e_f(ps, R_i)$

We propose a frame error rate computing algorithm based on single measurement, which is shown in algorithm 1, to avoid too much measurement cost, it can be divided into two steps:

(1) Evaluating channel SNR findSNR ($e_f(B_t,R_1),B_t,R_1$):

As shown in algorithm 2, estimating average SNR (Signal Noise Ratio) through statistic frame error rate, frame size, transmission rate and SNR-BER (signal noise ratio to bit error rate).

(2) Calculating frame error rate of transmission data findFER (snr,ps,R_i):

As shown in algorithm 3, we calculate frame error rate by average SNR, data size, transmission rate (from adaptive rate module) and SNR-BER.

```
Algorithm2. Calculation channel SNR of transmission data
     find SNR (e_f(B_t, R_1), B_t, R_1)
  Input: the test frame error rate e_f(B_t, R_1), the test frame size B_t, the test frame rate R_1 and the SNR-BER mapping table;
  Output: snr.
  1. Substitute e_f(B_t, R_1) and B_t into Eq. (5), e_f(B_t,R_1) = 1-(1-BER^1(snr))^24 (1-BER^{R_1}(snr))^{B_t} to calculate BER^{R_1}(snr)
  2. According to SNR-BER mapping table, BER^{R_1}(snr) and R_i, we obtain channel snr of data transmission
    3. Return snr
  Algorithm3. Frame error rate calculation algorithm with specified rate and packet size findFER (snr, ps, R_i)
  Input: the snr, the packet size ps, the send rate R_i, the SNR-BER mapping table
  Output: the frame error rate e_f(ps, R_i)
  1. According to snr and R_i, we can get bit error rate BER^{R_i}(snr) from SNR-BER mapping table
  2. Substitute BER^{R_i}(snr) and ps into Eq. (5), FER = 1-(1-BER^1(snr))^24 (1-BER^{R_i}(snr))^{ps}
    3. Return FER
```

Both algorithm 2 and algorithm 3 need to map the SNR into BER (bit error ratio). Some experiments and simulations have collected corresponding rate and channel error rate of IEEE 802.11a/b [22]. We employ SNR-BER mapping curve in [23] to obtain frame error rate via data frame size after SNR-BER mapping. As our previous work in [24], frame error rate is derived by:

$$e^m(L) = 1-(1-BER^m(snr))^L \tag{4}$$

where m is the modulation mode (transmission rate), L is the data length in bits, $BER^m(snr)$ is the bit error rate under the modulation mode m and the snr. From (4), combining with IEEE 802.11 MAC frame, we obtain frame error rate of length L under the modulation mode m as follows:

$$\begin{aligned} FER^m(L) &= 1-\left(1-e^1(24)\right)\left(1-e^m(L)\right) \\ &= 1-\left(1-BER^1(snr)\right)^{24}\left(1-BER^m(snr)\right)^L \end{aligned} \tag{5}$$

where $e^1(24)$ is the error rate of sending physical layer convergence protocol (PLCP). We can estimate channel SNR by sending a single probe frame, and then adopt frame size and transmission rate through SNR-BER mapping to estimate the frame error rate, consequently reduce the link measurement overhead. At the same time, combining Eqs. (3) and (5), we can calculate accurate airtime cost for different flows by considering the transmission rate and the specific traffic size.

3.3 Application differentiation from traffic flows

To meet the QoS requirements for SG's various applications in HWMP-NQ, we adopt the enhanced distributed channel access (EDCA) defined in IEEE802.11e [25] for QoS supporting. EDCA cache the upper service data in different queues with different access class (AC) to reflect different channel competition ability. These parameters include maximum/minimum contention window (CW_{max}/CW_{min}) and arbitration IFS number (AIFSN). The IEEE 802.11 [25] defined four ACs as shown in Table 1. They are AC_VO, AC_VI, AC_BE and AC_BK from high to low respectively.

For the i priority class, the contention window $CW_{i,j}$ in the j^{th} retransmission is calculated as:

$$CW_{i,j} = \min\left[2^j\left(CW_i^{\min}+1\right)-1, CW_i^{\max}\right], i\in 0, \ldots, N_c-1, j\in 0, \ldots, m \tag{6}$$

where N_c is the number of ACs with default value 4 and m is the maximum retransmissions with 4 or 7. Nodes can access channel until the channel has been idled for an $AIFS_i$ duration after back-off. The $AIFS_i$ can be calculated as:

$$AIFS_i = SIFS + AIFSN_i \times T_{slot} \tag{7}$$

Table 1 Smart grid applications and EDCA priority

Priority	AIFSN	CW_{min}	CW_{max}	QoS	Application type
0	2	7	15	AC_VO	Control information data
1	2	15	31	AC_VI	Demand response, Requested AMI, Power quality data
2	3	31	1,023	AC_BE	Meter reading data
3	7	31	1,023	AC_BK	Video surveillance

where *SIFS* is the short inter-frame space, and T_{slot} is the slot time. Eqs. (6) and (7) show that the higher the level of access (AC) is, the smaller contention window and the shorter AIFS are, and the faster channel access is. Therefore, we divide main NAN traffic into different levels as shown in Table 1. We use 1 bit in the QoS control field of packets to assign a latency tag (1 denote delay-tolerant). For example, video surveillance applications have a low priority but they are sensitive to delay. As shown in Fig. 1, if delay-sensitive traffic is marked with 0, they will be dropped directly over a certain time after checking the tag in the case of no alternative routes.

However, latency-tolerant traffic such as AMI data and periodic power quality data must be transmitted with the highest reliability and QoS support. Therefore, we design a delay-tolerant management module as shown in Fig. 1, which is under the assumption that AMI data and power quality data are not entirely time sensitive. For instance, we assume that AMI packets are transmitted every 15 s while power quality packets are transmitted every 3 s. As long as these packets are transmitted successfully within the interval, some delay variation is tolerable. The main focus of this module is using an extra queue to store packets that are labeled latency-tolerant and not be sent in time. If it has not a route or backup routes when we have packets to send, the delay-tolerant module will be triggered. First, the packet will be stored in a latency-tolerant queue if the tag bit is 1 (means delay-tolerant), then the next RANN (root announcement) period is initiated and the data in latency-tolerant queues will be transmitted if a valid route to the destination is resolved for the corresponding mesh STA. If the data failed to transmit resulting from channel collisions, EDCA will not discard the data but will hand it to the delay management model to wait for transmitting by available routes until timeout.

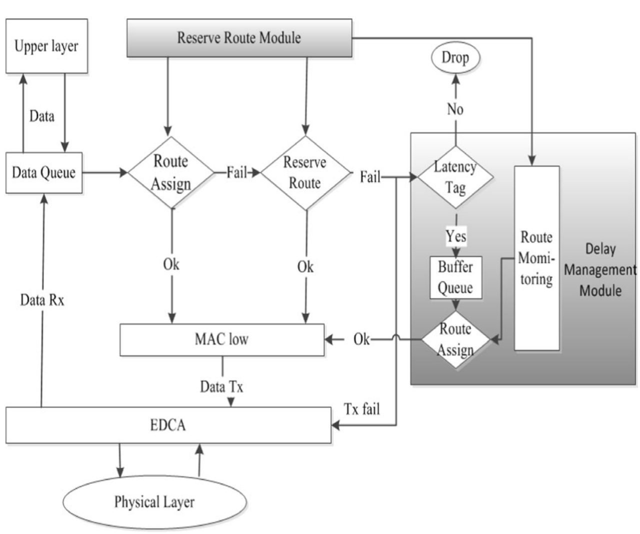

Fig. 1 Process block for different delay demand data

4 Routing reliability optimization

In order to improve the reliability of HWMP-NQ in SG environment, we mitigate the impact of routing oscillation via a multi-gateway backup routing scheme along with historical information. Furthermore, we develop a routing correction factor to rectify the impact of data transmission on routing overheads.

4.1 Multi-gateway backup routing selection

Wireless mesh nodes need to store routing entries to multiple gateways by collaborating with multi-gateway routing. We take the advantage of the MAC address of gateway to mark the tree routing of NAN to avoid the routing table conflict, then we add another routing table to reserve the suboptimal route to the same root or to other roots. In other words, a primary route with the minimum airtime cost is maintained in the primary routing table, and the alternate routing table save the suboptimal route to same root and routes to other x roots (x=2 in this paper). Nodes must ensure at least one available route to each gateway, no matter what the other routing criterion is, to guarantee the collaborations between neighbor area networks. Mesh STA (smart meter) will check the alternate routing table on whether there exists a route to the root when it receives a RANN massage coming from the root. If not, the mesh STA adds a new route entry with this RANN message. The mesh STA will update the corresponding route with this RANN information if already exists a route to this root in the routing table with a new sequence number or a better routing; otherwise the received RANN will be discarded. An example with three gateways is shown in Fig. 2. Node S maintains the minimal cost route (solid line) as the primary route and the rests as backup routes (dotted line) to different roots. In addition, with the one-hop PERR routing maintenance mechanism, a node does not transmit PERR message directly to the root when there is no reserved route or route fails. Instead, a PERR message is generated but only transmitted to one-hop neighboring mesh STAs which use the broken link. By taking the full advantage of the multi-gateway backup routing scheme, we can reduce the probability that a source node initiates the on-demand route discovery process by backtracking. Thus, we can achieve a higher reliability and efficiency in sharing the channel resources for SG, while the overhead is reduced.

4.2 Eliminating routing oscillation from historical information

Multi-gateway backup routing scheme selects optimal route to specific destination node through a route management module. Since using historical information can decrease the impact on network oscillations (such as those due to short-time signal

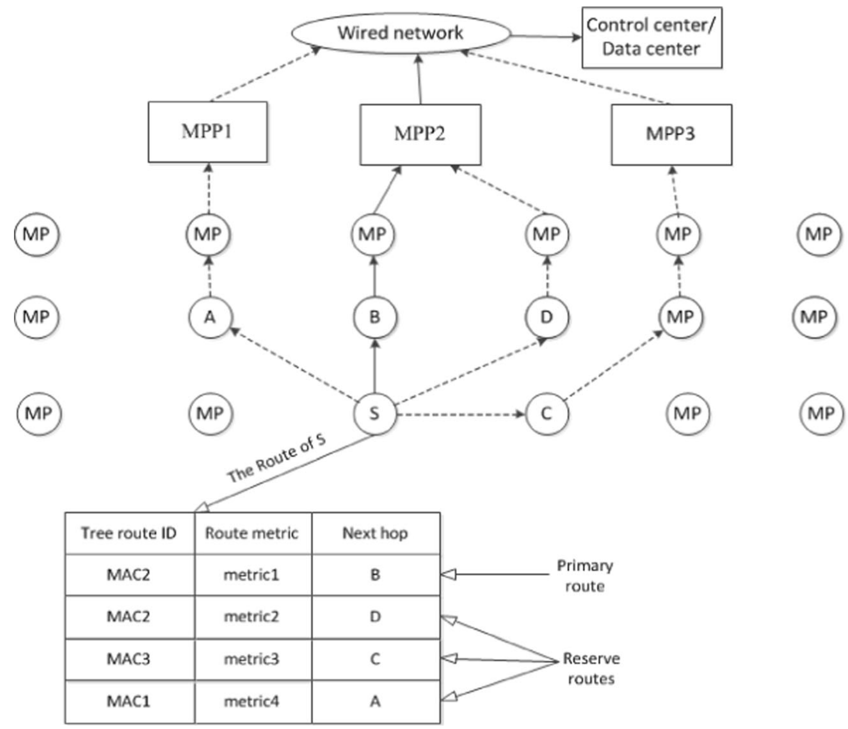

Fig. 2 Example of NAN with three gateways

interference, accidental packet loss, etc.) and make the route more stable and accurate. Hence, to improve the stability, each wireless node maintains the RANN information received in two consecutive RANN rounds (the current round and the previous round. Here a round is the time that the RANN information with a series of number traversals from the root node to all Mesh nodes).

Algorithm4. Multi-gateway backup routing selection

Input: the routing metric $C_a(n)$ of n round and the $C_a(n-1)$ of $n-1$ round, the primary route P_{curr} and the backup route P_{res} of $n-1$ round

Output: the primary route $P_{curr}(n)$ and the backup route

1. if $P_{curr}(C_a(n)) \leq \min[P_{res}(C_a(n)), P_{other}(C_a(n))]$
2. Select $P_{curr}(n-1)$ as $P_{curr}(n)$
3. else if $P_{curr}(C_a(n)-C_a(n-1))$□$\alpha \leq P_{res}(C_a(n)-C_a(n-1))$ and $P_{curr}(C_a(n))$□$\alpha + P_{curr}(C_a(n-1)) \leq P_{other}(C_a(n))$
4. Select $P_{curr}(n-1)$ as $P_{curr}(n)$
5. Select $\min[P_{res}(C_a(n)), P_{other}(C_a(n))]$ as $P_{res}(n)$
6. else
7. Select $\min[P_{res}(C_a(n)), P_{other}(C_a(n))]$ as $P_{curr}(n)$
8. Select the second-best in $\{P_{curr}(C_a(n)), P_{res}(C_a(n)), P_{other}(C_a(n))\}$ as $P_{res}(n)$

Each STA calculates link cost by using all received RANN messages, and a route with minimal cost is selected to transfer packets in current RANN round. The suboptimal route and the routes to other gateways will be stored in backup routing table as backup routes. As shown in algorithm 4, the link cost of the primary route and the backup routes will be stored as historical information in the next RANN round, and the latest link cost is computed via the latest RANN message simultaneously. If the link cost of the primary route is less than that of the backup routes in the new RANN round, the primary route is maintained. Otherwise, it will be updated with the corresponding measures.

In [21], mesh STAs compare the historical difference between the primary route and the backup routes when the link cost of the primary route is not minimal, and choose the one with the minimum historical difference as the new primary route to reduce routing oscillations. However, it ignores the case that the historical difference is quite small while the backup routes do not transfer data. Consequently, the historical difference of backup routes is much smaller than that of the primary route. In addition, it does not consider the effects of the current data transmission, and ignore other optimal paths except the primary route and reserved routes. Therefore, we introduce the routing correction factor α to involve the impact of current data transmission on the primary route when using historical information. At the same time, we compare it with optimal paths including but not limited to primary route and backup routes in a new RANN round, giving nodes the opportunity to choose more optimal route as shown in algorithm 4.3.

4.3 Routing correction factor

If the overhead of the primary route is not minimum in a new RANN round, whether we switch the route or not depends on the historical overhead differences between the primary route and the backup routes; meanwhile, it depends on the overhand comparisons of the primary route and the other routes. As shown in algorithm 4, the primary route switching should not satisfy the following two conditions:

(1) Minimum primary route historical difference:

$$P_{curr}(C_a(n)-C_a(n-1))\cdot\alpha\leq P_{res}(C_a(n)-C_a(n-1))$$

(2) When we consider the historical data, the primary route is superior to the other backup routes:

$$P_{curr}(C_a(n))\cdot\alpha+P_{curr}(C_a(n-1))\leq P_{other}(C_a(n))$$

When comparing historical difference, we want to eliminate the effects of the current data because it is not the interference flow. We have to consider the influence of other data flow for occupation transmission bandwidth and contention channel when comparing with other reserved routes, so we introduce the routing correction factor α that is the proportion of channel occupancy of data sent by all other routes expect the primary route, and it is calculated as follow:

$$\alpha=\frac{T-T(f)}{T} \quad (8)$$

where T is the channel occupancy time of transmitting all data flow in a RANN round, and $T(f)$ is the channel occupancy time of transmitting data flow f by primary route in a RANN round. In order to simplify the calculation and facilitate system development, we define the packet channel occupancy time as the transmission time of packet in the channel, regardless of the channel access time. Then, the channel occupancy time $t_{i,j}$ of packet j of the data flow i is calculated as:

$$t_{i,j}=\frac{ps_i}{R_{i,j}}\cdot n_{i,j} \quad (9)$$

where ps_i is the packet size of i data flow, we assume the packet size of the same traffic having a fixed value, $R_{i,j}$ is the transmission rate of j packet of flow i, and $n_{i,j}$ is the retransmission count. We can obtain the channel occupancy time T of all data in a RANN round by (9):

$$T=\sum_{i=0}^{N-1}\sum_{j=0}^{N_i-1}\frac{ps_i}{R_{i,j}}\cdot n_{i,j} \quad (10)$$

and $T(f)$ of flow f:

$$T=\sum_{j=0}^{N_f-1}\frac{ps_f}{R_j}\cdot n_j \quad (11)$$

where N is the total transmitted data in a RANN round, N_i is the total transmitted data in a RANN round of flow i and N_f is the total transmitted data of flow f in a RANN round.

5 Performance evaluation

Since the ns3[1] simulator includes IEEE 802.11 s module [26], we simulate and evaluate the HWMP-NQ protocol using ns3 and the original HWMP is used as routing protocol specification.

5.1 Experiments parameters setting

The simulation parameters are set as shown in Table 2. Each mesh node of NAN is equipped with IEEE 802.11a network interfaces, and we employ AARF as the adaptive rate adjustment algorithm. For each simulation setting, we repeat the simulation for 50 runs with different random seeds and take the average. We employ the same random number to compare different routing protocols in the same network environment (wireless link, flows, etc.).

In the simulation, the nodes are laid out in a grid topology and simulations are performed by using 3×3, 4×4, 5×5, 6×6, 7×7 and 8×8 NAN nodes with distance of 150 m between neighbor nodes. We add two mesh nodes into network as gateway nodes to gather the data of rest mesh nodes (smart meters). According to the communication requirements of smart grid, we configure the NAN data on ns3 as given in Table 3. In addition, we set random jitters for all periodic traffic to avoid neighbor nodes transmitting data simultaneously, and to reduce the impact of channel conflict on network performance.

[1] ns-3 Network Simulator 3. http://www.nsnam.org/

Table 2 Simulation environments

Parameter	Value
Simulation time	500 s
PHY standards	IEEE 802.11a
Transmitter power	18dbm
Wireless signal propagation delay model	Constant speed propagation delay model
Wireless signal propagation loss model	Log distance propagation loss model
Rate adaptive adjustment	Enable (AARF)
HWMP RANN interval	5 s
Numbers of simulation	50

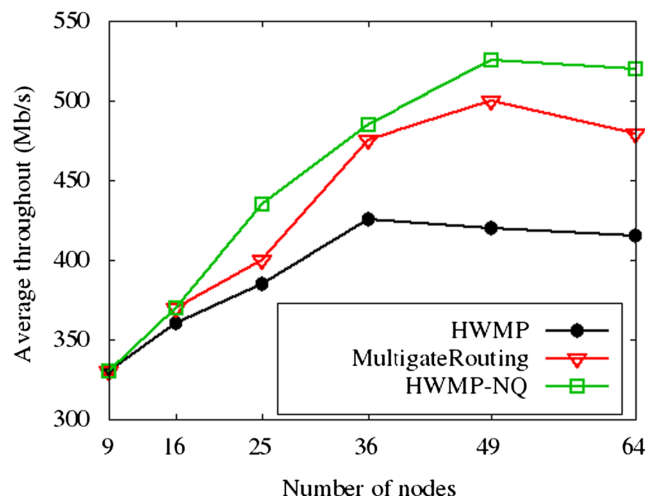

Fig. 3 Average throughout comparison of three protocols in various network sizes

5.2 Protocol comparison in NAN of different size

In the first experiment, we compare the performance of HWMP, Multi-gateway Routing [19] and HWMP-NQ protocols in different mesh network sizes (hereinafter, express in NS): 3×3 (9 nodes), 4×4 (16 nodes), 5×5 (25 nodes), 6×6 (36 nodes), 7×7 (49 nodes), 8×8 (64 nodes), respectively. We randomly add two mesh nodes as gateways aggregating NAN traffic data.

Figure 3 shows the average throughput that indicates the total amount of data received by each root node per second. As we can see, the increasing data makes the throughput increase and the network becomes congested with the number of nodes increasing. After certain saturation, the throughput begins to decrease since the increasing sizes of network leads to insufficient channel resources. The throughput of HWMP reaches saturation at NS=36, while the throughput of HWMP-NQ and Multi-gateway Routing reach the saturation at NS=49 due to better multi-gateway strategy. Besides, since HWMP-NQ is optimized for different SG NAN traffic, it could choose better transmission path to achieve a higher throughput than others.

Figure 4 shows the packet delivery ratio (PDR) that represents the ratio of total number of packets received by the root nodes and the overall number of packets transmitted by all NAN mesh nodes in the network. The network becomes increasingly congested and the PDR declines with the number of nodes increasing, especially, the PDR of HWMP decreases rapidly because of insufficient reliability. If we take $PDR \geq 90\%$ as the network standard, HWMP is only applicable to the network $NS \leq 25$ while Mitigate Routing is suitable to $NS \leq 36$. HWMP-NQ has the highest delivery ratio since it chooses better routes under different traffic flows and reduces the oscillation via multi-gateway backup route selection mechanism so that it can carry a higher amount of data and guarantee $PDR \geq 90\%$ when $NS \leq 49$.

The average end-to-end delay of each NAN's traffic is shown in Fig. 5. Since the optimized routing criterion and QoS service differentiation strategy are applied to HWMP-NQ for various NAN applications, it could choose a better route to achieve a lower end-to-end delay when $NS \leq 36$. When $NS > 36$, congestion starts to occur so that packets cannot be forwarded promptly, HWMP-NQ begins to deal with the important and delay-tolerate data by the latency-tolerate module rather than discarding it directly, so it has a higher delay but less than 100 ms which meets the traffic delay requirements. From Figs. 4 and 5 we can see that, HWMP-NQ guarantees the delay of NAN traffic and improves the PDR of NAN at the cost of a certain delay.

Table 3 Smart Grid applications set

Type of service	Application size	Transmission interval	Requirement latency	Priority (EDCA)	Latency tag bit
Periodic AMI	123 bytes	15 s	<15 s	2	1
AMI management	4,000 bytes	300 s	<1 s	0	0
Periodic power quality	3,000 bytes	3 s	<3 s	2	1
Power management	4,000 bytes	300 s	<1 s	0	0
Requested AMI	123 bytes	On-demand	<5 s	1	1
Requested power quality	2,000 bytes	On-demand	<5 s	1	1
Video surveillance	250kB/s	Constant	<100 ms	3	0

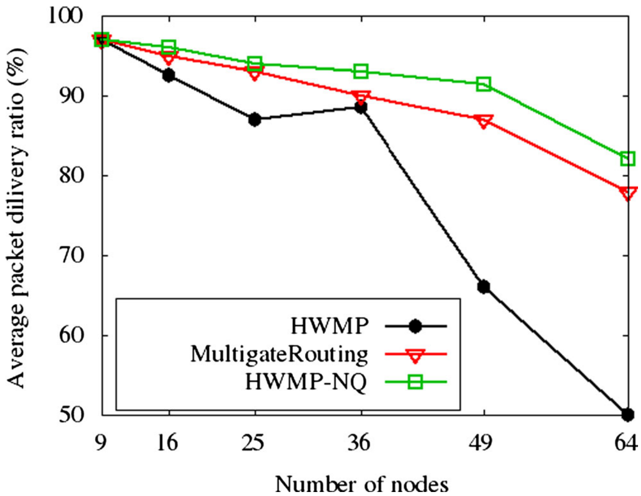

Fig. 4 Average packet delivery ratio comparison of three protocols in various network sizes

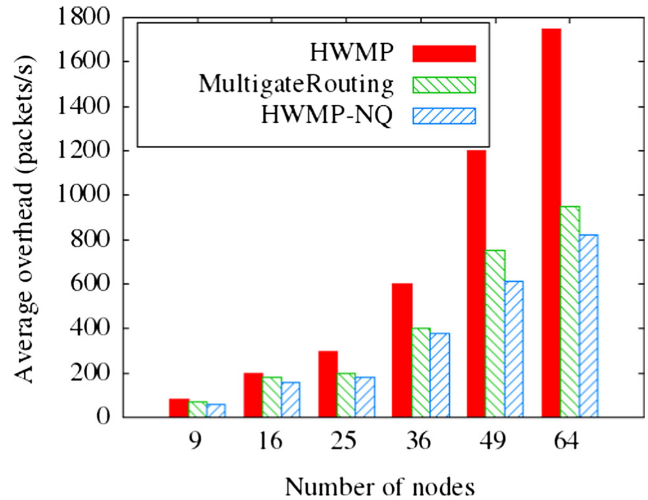

Fig. 6 Routing control information overhead comparison of three protocols in various network sizes

As Fig. 6 shows, the control messages (PERR and on-demand PREQ) generated in HWMP-NQ are reduced by nearly 60 % compare to HWMP when $NS=64$. That HWMP-NQ can significantly reduce the routing control messages is mainly due to three reasons. The first is that the optimized link cost metric allows better route selection, which results in fewer failed transmission packets. The second is that the multi-gateway backup routing scheme reduces the route oscillations, further improves the stability of the network and decreases the generation of PREQ packets. The last is that the single-hop PERR route maintenance mechanism reduces the PERR message sent when routing error occurred.

Figure 7 shows the comparison of packet delivery ratio (PDR) in various applications. HWMP, MR, NQ represent HWMP, Multi-gateway Routing, HWMP-NQ protocol respectively, and pe, re, vi respectively denote cycle data collection, on-demand request data, video surveillance data. As shown in Fig. 7, there are little PDR difference among each flow of HWMP and Multi-gateway Routing because they are not optimized for different NAN traffic so that they cannot guarantee the reliability of on-demand data, such as the requested AMI and power quality, when the network is congested. Since HWMP-NQ optimizes route criterion for NAN applications requiring different QoS to select the transmission route accurately for specific data. Moreover, it includes the priority queue strategy for different QoS requirements flows and the delay-tolerant module to ensure reliability for delay-tolerate traffic. Therefore, HWMP-NQ ensures the reliability of high priority traffic by sacrificing lower priority traffic when network is congested. The delivery rate of each flow is quite different. As shown in Fig. 7, packet delivery rate of on-demand request traffic (NQ pe) in HWMP-NQ has remained more than 90 %.

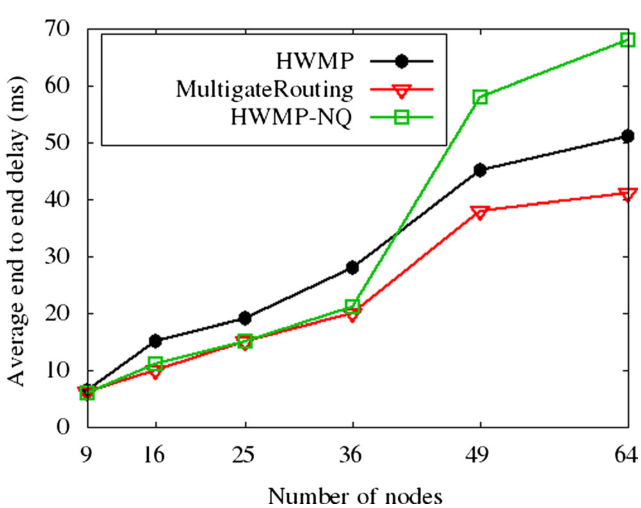

Fig. 5 Average end-to-end delay comparison of three protocols in various network sizes

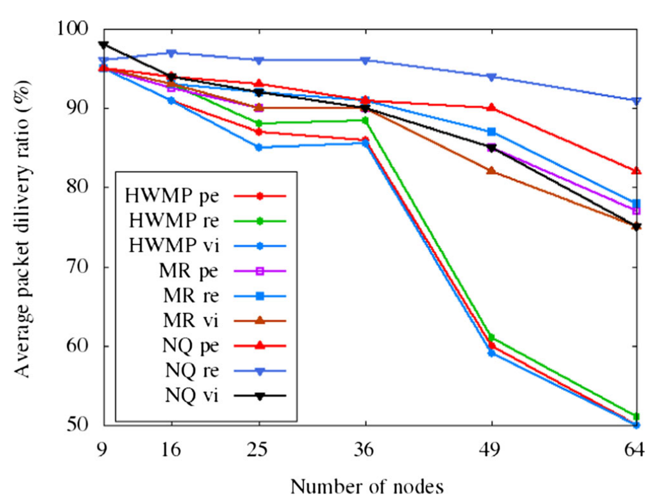

Fig. 7 Average packet delivery ratio of various NAN applications comparison in various network sizes

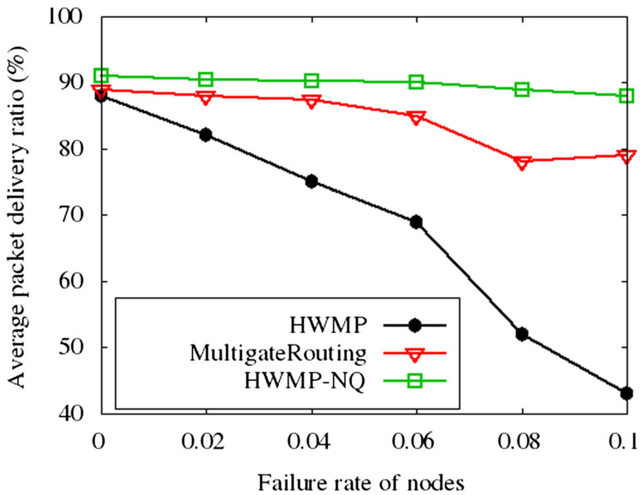

Fig. 8 Packet delivery ratio comparison of three protocols in various mesh node failure rate

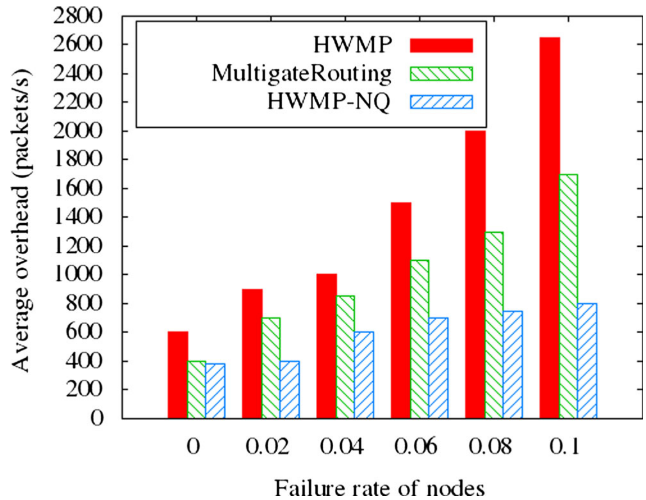

Fig. 10 Routing control information overhead comparison of three protocols in various mesh node failure rate

5.3 Network performance with mesh node failure rate

In the second experiment, we investigate the impact of wireless mesh node failure rate on network performance. We work with a fixed network topology *NS*=36 which the performance gaps are smaller between the three protocols according to the first experiment results to facilitate comparison. The failure rate (FR) for each node are set to [0, 0.1], and the simulation results are shown in Figs. 8, 9, 10 and 11.

Since the HWMP-NQ uses the multi-gateway backup route selection scheme, neighbor nodes could establish multi-hop routes to ensure the delivery ratio of critical data by using the alternate routing table when some neighboring mesh nodes are failed. We can see from Fig. 8, the packet delivery ratio of HWMP-NQ does not decline much and remains above 87 % with the increasing failure rate of mesh nodes. Comparing to HWMP and Multi-gateway Routing, HWMP-NQ always has the highest delivery rate, while HWMP will discard data at each failure node or failure link, which leads to data delivery rate decrease rapidly. Multi-gateway Routing can effectively reduce the influence of mesh nodes fault on data transmission through multi-gateway coordination mechanism to establish a new transmission path to some extent.

As shown in Fig. 9, since HWMP drops packets directly when a node fails, and then notifies the source node to broadcast PERR messages and tries to find the path to re-send data, the average end-to-end delay quickly becomes larger with the failure rate of mesh nodes increasing. Multi-gateway routing effectively reduces the latency growth with the gateway load scheduling mechanism based on back-pressure when nodes failure happened, hence the delay is minimum. Despite sacrificing end-to-end transmission delay to ensure packet delivery ratio of delay tolerate traffic, HWMP-NQ employs alternate routes of neighbors to build new path through multi-gateway backup route selection scheme and PERR based single-hop route maintenance mechanism, which avoids on-demand route discovery delay

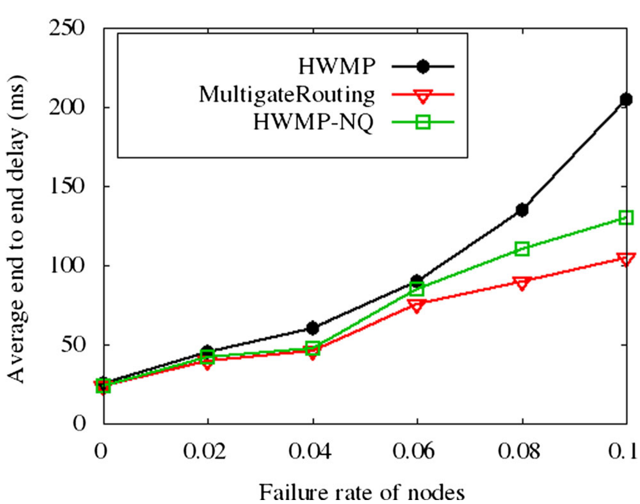

Fig. 9 End-to-end delay comparison of three protocols in various mesh node failure rate

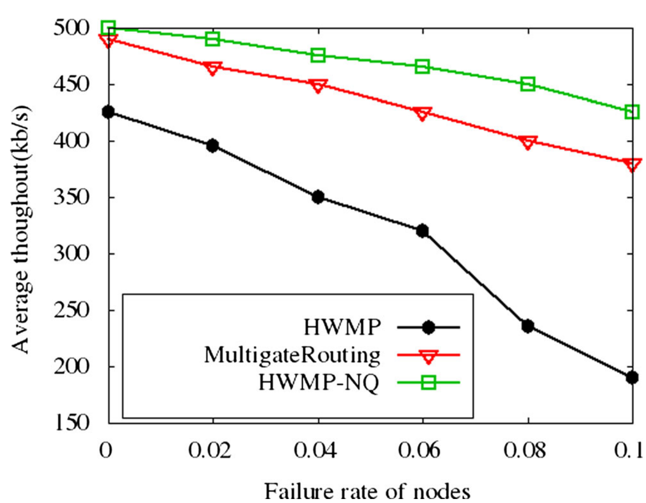

Fig. 11 Throughout comparison of three protocols in various mesh node failure rate

overhead so that to achieve a lower transmission delay than HWMP at a higher failure rate ($FR \geq 0.02$).

We can see from Fig. 10, HWMP-NQ makes full use of neighbors backup routes information to build multi-hop routing and retransmit data through single-hop PERR mechanism, which reduces the probability of triggering source node on-demand routing discovery process and greatly decreases the PERR and on-demand PREQ packet transmission frequencies in the mesh nodes fault (routing error) case. Since HWMP-NQ reduces routing control information overhead, NAN traffic has more network resources to use. Therefore, as shown in Fig. 11, HWMP-NQ can maintain high average throughput even facing increasing failure rate of mesh nodes.

6 Conclusion

In this paper, we have presented a NAN QoS-aware routing scheme, called HWMP-NQ, for optimizing HWMP protocol to meet the QoS requirements and improve the reliability for smart grid. The HWMP-NQ not only improves the accuracy of routing criterion and reflects the characteristics of different SG applications by modifying the airtime cost metric of HWMP that considers the data size and transmission rate. But also reduces the overhead of link measurements through the single measurement based traffic QoS calculation algorithm, and meets the QoS requirements of smart grid through the QoS-based service differentiation strategy. In addition, the reliability of HWMP-NQ has been improved by utilizing a multi-gateway backup routing scheme. Simulation results have demonstrated that the proposed HWMP-NQ shows higher performance than other existing schemes in terms of average packet delivery ratio, end-to-end delay, routing control information overhead and throughput, even facing a high failure rate of mesh nodes. In our future work, we will focus on data fusion on gateways which are equipped with multi-radio multi-channel to reduce access channel overhand and interference so as to improve reliability of smart grid communication networks preferably.

Acknowledgments The authors acknowledge the support of National Natural Science Foundation of China projects of grant No. 61379058, 61379057, 61350011, 60903058, and Natural Science Foundation of Hunan Province project of grant No.10JJ6093.

References

1. Farhangi H (2010) The path of the smart grid. IEEE Power Energy Mag 8:18–28
2. Gungor VC, Lambert FC (2006) A survey on communication networks for electric system automation. Comput Netw 50:877–897
3. Liu A, Jin X, Cui G, Chen Z (2013) Deployment guidelines for achieving maximum lifetime and avoiding energy holes in sensor network. Inf Sci 230:197–226
4. Liu A, Ren J, Li X, Chen Z, Shen X (2012) Design principles and improvement of cost function based energy aware routing algorithms for wireless sensor networks. Comput Netw 56(7):1951–1967
5. Dong M, Ota K, Li X, Shen X, Guo S, Guo M (2011) Harvest: a task-objective efficient data collection scheme in wireless sensor and actor networks. CMC 2011:485–488
6. Dong M, Ota K, Yang LT, Chang S, Zhu H, Zhou Z (2014) Mobile agent-based energy-aware and user-centric data collection in wireless sensor networks. Comput Netw 74:58–70
7. Fang X, Misra S, Xue G (2012) Smart grid – the new and improved power grid: a survey. IEEE Commun Surv Tutor 14:944–980
8. Wu J, Dong M, Ota K, Zhou Z, Duan B (2014) Towards fault-tolerant fine-grained data access control for smart grid. Wirel Pers Commun 75(3):1787–1808
9. Fan Z, Kulkarni P, Gormus S, Efthymiou C, Kalogridis G, Sooriyabandara M, Zhu Z, Lambotharan S, Chin WH (2013) Smart grid communications: overview of research challenges, solutions, and standardization activities. IEEE Commun Surv Tutor 15:21–38
10. IEEE 802.11s, "Part 11: Wireless LAN Medium Access Control (MAC) and Physical Layer (PHY) specifications Amendment 10: Mesh Networking", 2011
11. L. H and Z. W, (2010) "QoS Routing in Smart Grid," Global Telecommunications Conference (GLOBECOM 2010), pp. 1–6
12. Gui J, Liu A (2012) A new distributed topology control algorithm based on optimization of delay and energy in wireless networks. J Parallel Distrib Comput 72:1032–1044
13. Chen FZZ (2009) Cost-sensitive and load-balancing gateway placement in wireless mesh networks with QoS constraints. J Comput Sci Technol 24:775–785
14. Xu Y, Wang W (2013) Wireless mesh network in smart grid: modeling and analysis for time critical communications. IEEE Trans Wirel Commun 12:3360–371
15. T. Iwao, K. Yamada, M. Yura, Y. Nakaya, A. A. Cardenas, S. Lee, and R. Masuoka, (2010) "Dynamic Data Forwarding in Wireless Mesh Networks," 2010 I.E. 1st International Conference on Smart Grid Communications (Smartgridcomm), pp. 385–390
16. S. Dawson-Haggerty, A. Tavakoli and D. Culler, (2010) "Hydro: A Hybrid Routing Protocol for Low-Power and Lossy Networks," 2010 I.E. 1st International Conference on Smart Grid Communications (SMARTGRIDCOMM), pp. 268–273
17. Dong M, Kimata T, Sugiura K, Zettsu K (2014) Quality-of-experience (QoE) in emerging mobile social networks. IEICE Trans 10:2606–2612
18. D. De Couto, D. Aguayo, J. Bicket, and R. Morris, "A high-throughput path metric for multi-hop wireless routing,", MobiCom, Ed.: ACM, 2003, pp. 134–146
19. Gharavi H, Hu B (2011) Multigate communication network for smart grid. Proc IEEE 99:1028–1045
20. J. Ji-Sun, L. Keun-Woo, K. Jae-Beom, K. Young-Bae, K. Younghyun, and L. Sang-Yeom, (2011) "Improving IEEE 802.11s Wireless Mesh Networks for Reliable Routing in the Smart Grid Infrastructure," in Communications Workshops (ICC), 2011 I.E. International Conference on, Kyoto, pp. 1–5
21. Kim J, Kim D, Lim K, Ko Y, Lee S (2012) Improving the reliability of IEEE 802.11 s based wireless mesh networks for smart grid systems. J Commun Netw 14:629–639
22. Trivellato M (2005) Windowed/shaped OFDM and OFDM-OQAM: alternative multicarrier modulations for wireless applications. University of Padova, Italy
23. J. D. Pavon and S. Choi, (2003) "Link adaptation strategy for IEEE 802.11 WLAN via received signal strength measurement," *NEW YORK: IEEE*, pp. 1108–1113
24. D. Xiaoheng, L. Xu, L. Qiang, and C. Zhigang, (2013) "Link Adaptation Scheme with Signal-to-Noise Ratio Feedback for IEEE 802.11 Networks," in High Performance Computing and

Communications & 2013 I.E. International Conference on Embedded and Ubiquitous Computing (HPCC_EUC), 2013 I.E. 10th International Conference on, Zhangjiajie, pp. 1281–1286
25. IEEE 802.11, "Wireless LAN medium acess control(MAC) and physical layer(PHY) specification," 2012
26. A. K and B. P, (2010) "IEEE 802.11 s mesh networking NS-3 model, " Workshop on ns3, vol. 43

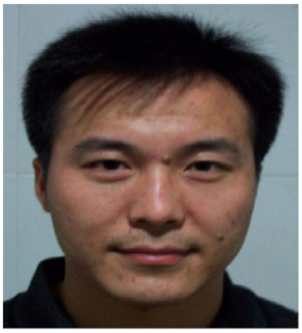

Xiaoheng Deng received the Ph.D. degrees in computer science Central South University, Changsha, Hunan, P.R. China, in 2005. Since 2006, he has been an Associate Professor and then a Full Professor with the Department of Electrical and Communication Engineering, Central South University. He is a senior member of CCF, a member of CCF Pervasive Computing Council, a member of IEEE and ACM. He has been a chair of CCF YOCSEF CHANGSHA from 2009 to 2010. His research interests include wireless communications and networking, congestion control for wired/wireless network, cross layer route design for wireless mesh network and ad hoc network, online social network analysis.

Lifang He is a M.Sc. student in School of Information Science and Engineering of Central South University, Changsha, China. She received the B.Sc. degrees in electronic and information engineering from Kunming University of Science and Technology, Kunming, China, in 2013. Her major research interests are wireless mesh network and smart grid.

Xu Li CCF member, received his M.Sc. degrees in Information Science and Engineering of Central South University, Changsha, China, in 2014. His research interests include cross-layer design in routing metric and protocol of wireless mesh network and MAC layer.

Qiang Liu CCF member, received the M.Sc. degrees in Information Science and Engineering of Central South University, Changsha, China, in 2014. His research interests include the routing protocol design and channel assignment of the wireless mesh network.

Lin Cai (S'00–M'06–SM'10) received the M.A.Sc. and Ph.D. degrees in electrical and computer engineering from the University of Waterloo, Waterloo, ON, Canada, in 2002 and 2005, respectively. Since 2005, she has been an Assistant Professor and then an Associate Professor with the Department of Electrical and Computer Engineering, University of Victoria, Victoria, BC, Canada. She has been an Associate Editor for the IEEE TRANSACTIONS ON WIRELESS COMMUNICATIONS, the IEEE TRANSACTIONS ON VEHICULAR TECHNOLOGY, the EURASIP *Journal on Wireless Communications and Networking*, the *International Journal of Sensor Networks*, and the *Journal of Communications and Networks*. Her research interests include wireless communications and networking, with a focus on network protocol design and control strategy supporting emerging applications in ubiquitous networks.

Zhigang Chen He received B.Sc. the M.Sc. and Ph.D degrees from Central South University, China, 1984, 1987 and 1998, Heis a Ph.D. Supervisor and his research interests are in network computing and distributed processing.